Structure-Transport Relationship in Organized Soft Matter Systems by Diffusion NMR

Eric Hazelbaker, Aakanksha Katihar, Monica Sanders, Amrish Menjoge, and Sergey Vasenkov

University of Florida, Department of Chemical Engineering, 423 ChE Bldg., Gainesville, FL 32611, USA

Corresponding author:
Sergey Vasenkov
Dept. of Chemical Engineering
University of Florida
Gainesville, FL 32611
E-Mail: vase17@ufl.edu

Abstract

In this paper we demonstrate and discuss the potentials of pulsed field gradient nuclear magnetic resonance (PFG NMR) at high magnetic field and high magnetic field gradients for uncovering the relationship between the structural and transport properties of soft matter systems. The reported diffusion studies are focused on room temperature ionic liquids and their mixtures with carbon dioxide or water as well as on multicomponent lipid bilayers. Both types of systems exhibit a well-defined structural organization on various length scales. Our experimental approach allows correlating this structural organization with the transport properties. The diffusion data were obtained by proton and carbon-13 PFG NMR. The experimental studies were in some cases complemented by dynamic Monte Carlo simulations.

1. Introduction

Room temperature ionic liquids (RTILs) are organic salts that are liquid at temperatures around room temperature. RTILs are gaining attention of the scientific community due to their potential applications as a media for organic synthesis, catalytic reactions, separation processes, extraction, etc. [1, 2]. A well-defined nanostructural organization of RTILs, which is manifested by the formation of polar and nonpolar domains, is believed to be responsible for many useful properties of these solvents. Aggregation of molecules into various types of domains also determines many properties of other types of soft matter systems such as multicomponent lipid bilayers. In particular, lipid diffusion along the bilayer plane can be drastically altered by the formation of lipid domains or rafts [3-11]. Fundamental knowledge of an influence of domain formation and aggregation on transport properties can be obtained by using a pulsed field gradient (PFG) NMR technique that combines advantages of high field (17.6 T) NMR and high

magnetic field gradients (up to 30 T/m) [12]. This technique has been recently introduced at the University of Florida in collaboration with the National Magnet Lab.

High field and high gradient PFG NMR was used to carry out diffusion studies of several imidazoluim-based ionic liquids and their mixtures with carbon dioxide or water. This technique was also applied for investigations of lateral lipid transport in multicomponent lipid bilayers with and without membrane domains. In addition to a more conventional ^{1}H PFG NMR, also ^{13}C PFG NMR was used. For the interpretation of the PFG NMR results obtained for lipid bilayers the experimental data were compared with the corresponding results of dynamic Monte Carlo simulations of lipid diffusion.

2. Experimental

^{1}H and ^{13}C PFG NMR diffusion studies were carried out using a wide bore 17.6 T Bruker Biospin spectrometer. Magnetic field gradients were generated using diff60 diffusion probe (Bruker Biospin) and Great60 gradient amplifier (Bruker Biospin). In most cases diffusion studies were performed by using the standard PFG NMR stimulated echo pulse sequence with and without eddy current delay. The absence of disturbing susceptibility effects and other measurement artifacts was confirmed by using the following strategies: (i) the results obtained by the stimulated echo PFG NMR sequence were confirmed by comparing these results with the corresponding data obtained by the 13-interval PFG NMR sequence with bipolar gradients [13]; (ii) it was verified that the diffusion data obtained at different magnetic field amplitudes (and otherwise under the same conditions) were the same within the experimental uncertainty, and (iii) proton and carbon-13 PFG NMR diffusion data measured for the same diffusing species in the same samples and under the same conditions were found to coincide within the experimental uncertainty. The PFG NMR signal intensity was determined by integrating the area under selected line(s) of the spectra recorded by a PFG NMR pulse sequence or by using the amplitudes of these line(s). Different lines in such spectra can correspond to different species. Hence, diffusion data for a chosen type of species in a sample can be obtained by selecting an appropriate line in the spectrum for data processing. For NMR lines originating from the diffusing species in the same types of local environment/domains and exhibiting no significant overlap with the lines of other types of ions or molecules in a sample the diffusivity (D) was determined from the signal attenuation $\left(\Psi \equiv A(g) \big/ A(g=0) \right)$ measured by the PFG NMR stimulated echo pulse sequence

$$\Psi = \exp\left(-(\gamma \delta g)^2 D t_{eff}\right), \qquad (1)$$

where γ is the gyromagnetic ratio, δ denotes the effective duration for rectangular gradient pulses, g is the amplitude of the magnetic gradients, t_{eff} is the effective diffusion time ($t_{eff} = \Delta - \delta/3$), and Δ is the separation between the gradient pulses. When a selected NMR line has contributions either from species in different types of domains or from different types of molecules and/or ions having different diffusivities the attenuation curves were described as a sum of two or three weighted exponential terms of the type shown in Eq.1

$$\Psi = \sum_{i=1}^{n=2or3} A_i \exp\left(-\left(\gamma\delta g\right)^2 D_i t_{eff}\right), \qquad\qquad (2)$$

where A_i and D_i represent, respectively, the fraction and diffusivity of ensemble i. The signal attenuation was measured under the conditions when only the value of g was varied and all other parameters in the PFG NMR stimulated echo sequence remained constant.

PFG NMR samples for studies of diffusion in RTILs with and without water and in lipid bilayers were prepared as discussed in Refs. [12, 14]. The samples of RTIL mixtures with carbon-13 labelled CO_2 were prepared in a similar manner. Briefly, the samples were prepared by filling 5 mm NMR tube with a chosen RTIL. In all cases the sample height in a vertically-oriented tube was around 12 mm or smaller to prevent disturbing influence of convection effects on the data measured at elevated temperatures. The RTIL samples were dried and loaded with CO_2 using a custom-made vacuum system. The removal of water from RTILs was performed by keeping them at elevated temperatures under high vacuum for at least 1 day. The loading was performed either by exposing a dry liquid to CO_2 gas at a fixed pressure for at least 4 hours or by freezing CO_2 from the calibrated volume of the vacuum system into the NMR tube with the sample using liquid nitrogen. The NMR tubes were flame-sealed after loading was complete.

The multibilayer stacks for diffusion studies were prepared from ternary lipid mixtures of 1,2-dioleoyl-sn-glycero-3-phosphocholine (DOPC), 1,2-dipalmitoyl-sn-glycero-3-phosphocholine (DPPC), and cholesterol (CHOL). The stacks were supported on thin glass plates. The lipid orientation in bilayers was confirmed using ^{1}H and ^{31}P NMR. For ^{1}H PFG NMR diffusion studies the stacks were oriented in the magnet bore at the magic angle to reduce disturbing influence of the dipole-dipole interactions on the measured proton signal.

3. Results and Discussion

3.1 Self-diffusion in mixtures of RTILs with CO_2 and water

^{13}C and ^{1}H PFG NMR was used to study the influence of an absorption of carbon dioxide and water into RTILs on the ion diffusion. In addition, the diffusion of CO_2 and water in mixtures of RTILs with carbon dioxide or water was also studied. Fundamental understanding of transport properties of mixtures of RTILs with carbon dioxide is essential for potential applications of RTILs for CO_2 separations. Such applications are feasible in view of the recent results indicating that the absorption capabilities of RTILs for CO_2 can be quite high [15-19]. To our knowledge, until now all diffusion studies of CO_2 in RTILs reported in the literature were performed by "macroscopic" techniques, which are based on measurements of gas fluxes through macroscopic IL samples [20-22]. Here we present the CO_2 diffusion data that were obtained by microscopic self-diffusion measurements of mixtures of an RTIL and CO_2 by ^{13}C PFG NMR. Fig. 1a shows the results of such measurements for a mixture of 1-n-butyl-3-methylimidazolium bis(trifluoromethylsulfonyl)imide ([bmim][Tf2N]) and ^{13}C-labelled CO_2. Owing to a superior sensitivity of our high field PFG NMR technique, in addition to ^{13}C PFG NMR

attenuation curves of ^{13}C-labelled CO_2 it was possible to measure the corresponding attenuation curves for the [bmim] cation and [Tf2N] anion by natural abundance ^{13}C PFG NMR (Fig.1). All attenuation curves in Fig.1a are monoexponential in agreement with Eq.1. Fitting the attenuation curves in Fig.1a by this equation resulted in the following diffusivities at 297 K: 3.9×10^{-11} m^2/s for the [bmim] cation, 3.1×10^{-11} m^2/s for the [Tf2N] anion, and 5×10^{-10} m^2/s for CO_2. It is important to note that the CO_2 diffusivity reported above for a mixture of [bmim][Tf2N] and CO_2 is much lower than that of CO_2 dissolved in traditional organic solvents. This observation can be explained by a relatively low mobility of ions that surround CO_2 molecules in the RTIL.
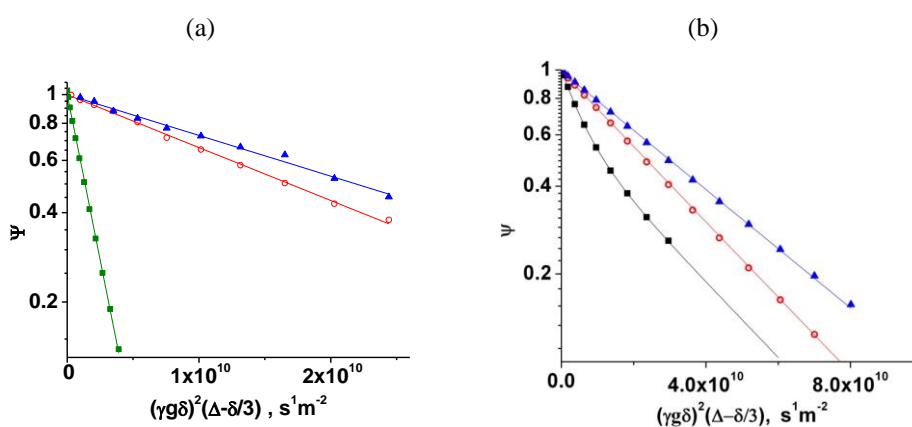
Figure 1: (a) Carbon-13 PFG NMR attenuation curves measured for the sample of [bmim][Tf2N] loaded with ^{13}C-labelled CO_2. The carbon dioxide loading corresponds to 0.15 carbon dioxide molecules per anion-cation pair. The attenuation curves were measured for effective diffusion time of 8.6 ms at T = 297 K. The data are shown for the average of the [bmim] lines at 129.4, 42.3, 24.3, and 11.7 ppm (○), the average of the [Tf2N] lines at 113.6 and 111.9 ppm (▲), and the carbon dioxide line at 117.6 ppm (■). Solid curves show the best fit results using Eq. 1. (b) Proton PFG NMR attenuation curves measured for the sample of [emim][EtSO4] containing 7% (w/w) water for t_{eff} = 49.3 ms at T = 288 K. The data are shown for the [emim] line at 1.5 ppm (○), the [EtSO4] line at 1.2 ppm (▲), and the water line at 4.2 ppm (■). The latter line has a contribution from the [emim] lines centered at 4.38 and 4.07 ppm. Solid curves show the best fit results using Eq. 1 for the cation and anion and using Eq. 2 with n = 2 for water. Eq. 2 was used due to the existence of an overlap between the water and [emim] lines

In addition to carbon dioxide, RTILs can also easily absorb large amounts of water. Studies of an influence of water on dynamic and structural properties of RTILs are important because water is usually present in various industrial streams. Fig. 1b shows examples of the measured proton PFG NMR attenuation curves in 1-ethyl-3-methylimidazolium ethylsulfate ([emim][EtSO4]) containing 7% (w/w) water. It is seen that the attenuation curves for the ions are monoexponential, while that for water shows large deviations from the monoexponential behaviour. These deviations are related to an

existence of an overlap between the water line and the lines of the [emim] cation in the measured NMR spectrum [14]. Fitting the attenuation curves of the pure cation and anion lines by Eq. 1, and the attenuation curve of the water line partially overlapping with the cation lines by Eq. 2 with n = 2 corresponding to the water and cation diffusivities (Fig. 1b) resulted in the following diffusivities at 25 C: 4×10^{-11} m^2/s for the [emim] cation, 3×10^{-11} m^2/s for the [EtSO4] anion, and 2×10^{-10} m^2/s for H_2O.

Figs. 2a and b show the dependencies of the diffusivities in the mixtures of RTILs with carbon dioxide or water on the concentrations of carbon dioxide or water. It is seen that the absorption of both carbon dioxide and water into RTILs increases the diffusivities of the cations and anions forming these RTILs.
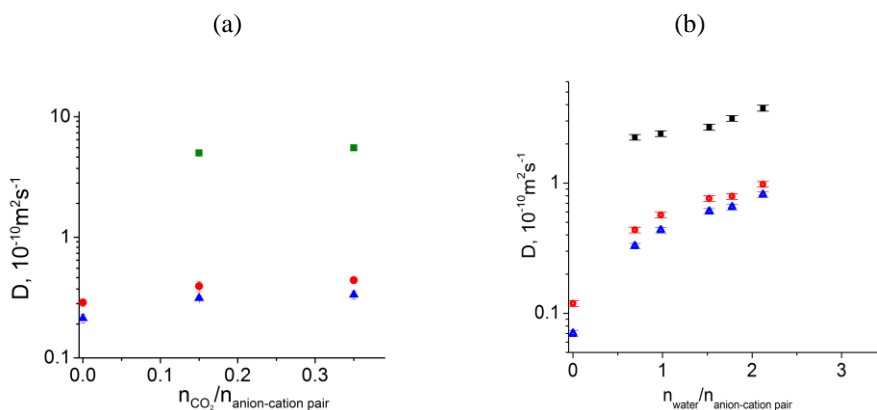
Figure 2: (a) Diffusivities of the [bmim] cation (●), [Tf2N] anion (▲), and CO_2 (■) measured by carbon-13 PFG NMR as a function of the number of CO_2 molecules per anion-cation pair in [bmim][Tf2N] at 297 K. (b) Diffusivities of the [emim] cation (●), [EtSO$_4$] anion (▲), and water (■) measured by proton PFG NMR as a function of the number of water molecules per anion-cation pair in [emim][EtSO4] at 298 K.

A disruption of a well-defined local order in the mutual arrangements of the cations and anions by CO_2 or water molecules is believed to be responsible for the observed concentration dependencies of the ion diffusion coefficients. The results in Fig. 2b show that an addition of water into an RTIL can change the relationship between the diffusivities of the cations and the anions. While in the water-free RTIL the diffusivity of a larger [emim] cation was observed to be greater than that of a smaller [EtSO4] anion, this anomalous relationship between the size and diffusivity of the diffusing species was found to become much less pronounced with an addition of water into the RTIL [14, 23]. Such behaviour is attributed to the existence of well-defined local structures in the pure RTIL resulting in an appearance of diffusion anisotropy for the cation diffusion. At the same time, these structures do not lead to significant diffusion anisotropy for the anion. With increasing water concentration these structures are believed to become progressively less well defined leading to a change towards "normal" relationship between the size and diffusivity of diffusing species [14, 23]. In contrast to water, the

absorption of carbon dioxide into the studied RTIL did not result in any significant changes in the relationship between the diffusivities of the cation and anion (Fig.2a).

3.2 Exchange of lipid molecules between membrane domains and their surroundings in planar multibilayer stacks

Membrane domains (or rafts) represent an important type of structural heterogeneity of cell membranes and of the corresponding model membranes. Such domains are characterized by an enhanced concentration of cholesterol, sphingolipids and certain types of proteins. Obtaining fundamental knowledge on the diffusion-driven exchange of lipid molecules between membrane domains and their surroundings in multicomponent lipid membranes is important for a number of biomedical and bioengineering applications ranging from drug delivery through cell membranes to the development of new biomedical technologies and therapies. Here we demonstrate the potential of high field and high gradient PFG NMR to directly monitor lipid exchange between such domains and surrounding areas of membranes. It was found that the proton PFG NMR attenuation curves measured for DOPC and DPPC in the planar DOPC/DPPC/CHOL multibilayer stacks can be described by Eq. 2 with n = 2 corresponding to the lipid diffusion inside and outside of membrane domains. It is important to note that under our experimental conditions both DOPC and DPPC lipids diffuse with the same diffusivity in the same type of the membrane environment. Hence, only two lipid components with different diffusivities were observed. Figure 3 illustrates the diffusion behaviour of these components at small (14 ms) and large (179 ms) values of the effective diffusion time for $T = 301.6$ K, which is close to the transition temperature corresponding to the onset of the domain formation.
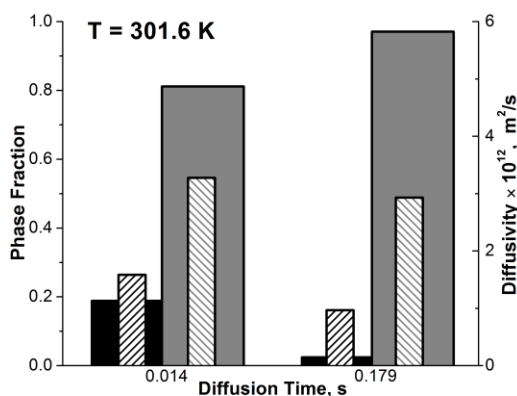
Figure 3: Comparison of diffusion behavior for different effective diffusion times in DOPC/DPPC/CHOL multibilayer stacks. The amplitudes of the solid columns show the phase fractions (left vertical axis) of the lipids diffusing inside the membrane domains (black) and outside the domains (grey) while the amplitudes of the striped columns correspond to the diffusivities (right vertical axis) of the lipid ensembles indicated by the solid columns they are superimposed on.

It is seen in the figure that the fraction of molecules attributed to the diffusion inside the domains decreases with an increase in effective diffusion times. This indicates an existence of lipid exchange between the domains and their surroundings. At the larger diffusion time, most lipids diffuse either outside the domains or diffuse a fraction of the diffusion time inside the domains and the remaining fraction of diffusion time outside the domains. Since the lipid diffusivity outside the domains is ~2 times larger than that inside the domains, lipids that spend a significant fraction of the observation time outside the domains will be attributed to the ensemble diffusing outside the domains. At smaller diffusion time there is no or insignificant lipid exchange between the domains and their surroundings.

Comparison of the experimental data on the lipid exchange with the corresponding results of dynamic Monte Carlo (MC) simulations allowed estimating the permeability of the domain boundaries. In these simulations lipid diffusion was modelled by random walk on square lattices containing low lateral mobility domains that were surrounded by areas with larger lateral diffusivities corresponding to those in the areas outside of the domains in the experimentally studies membranes. The simulations details and the procedure of fitting PFG NMR results by the corresponding results of simulations to estimate permeabilities of the domain boundaries and domain sizes in lipid membranes were recently reported in [12]. Similar approach has also been used earlier to estimate the permeability of the external surface of microporous crystals [24-26].

Fig. 4 shows dependencies of the relative number of lipid molecules, γ, which at initial time ($t = 0$) have started their trajectories inside the domains and were outside these domains by the time shown on the horizontal axis of the figure.
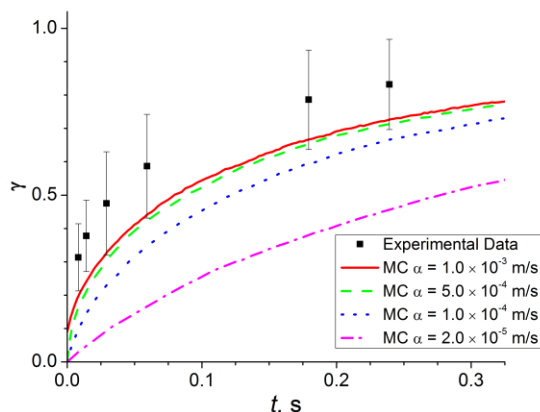
Figure 4: Examples of the dependencies of the normalized fraction of molecules that started their trajectories inside membrane domains and ended their trajectories outside of domains (γ) on diffusion time. Points and lines show the PFG NMR data and the results of dynamic MC simulations, respectively. The results of MC simulations are shown for different permeabilities of the domain boundaries (α). Experimental data was obtained at 301 K.

Such dependencies are often referred to as tracer exchange curves. The data in Fig. 4 were obtained from the PFG NMR measurements described above and also from the MC

simulations, which were performed for different permeabilities of the domain boundary, α. The values of α in Fig. 4 correspond to a range between the limiting case when the domain boundary provides no additional transport barriers for lipid molecules (1.0×10^{-3} m/s), and a value of α which is almost two orders of magnitude smaller (2.0×10^{-5} m/s). It is seen in Fig. 4 that within the experimental uncertainty, the experimental data agrees with the simulation results obtained for $\alpha \geq 5.0 \times 10^{-4}$ m/s. Hence, our results show that close to the transition temperature domain boundaries do not slow down lipid exchange between membrane domains and the surrounding areas of lipid membranes. Using the relationship between the length scales in the experiment and simulations as well as the domain size used in the simulations we estimate the domain radius to be 930 ± 290 nm at 301 K [12].

4. Conclusion

The results reported above demonstrate that PFG NMR at high magnetic field and high gradients allow obtaining deep insights into relationship between transport properties of molecules or ions in soft matter systems and formation of domains or aggregates in these systems. In particular, a partial breakdown of a well-defined local order in RTILs due to absorption of carbon dioxide or water was shown to lead to an increase of ion diffusivities. It was also demonstrated that water addition to an RTIL can change the relationship between the cation and anion diffusivities. High field and high gradient PFG NMR was used to directly monitor exchange of lipids between membrane domains and their surroundings in planar multibilayer stacks. The comparison of the experimental tracer exchange curves with the corresponding results of dynamic MC simulations allowed estimating the permeability of the domain boundaries and the domain sizes.

Acknowledgements

References

[1]   T. Welton, Chemical Rev., 99 (1999) 2071-2083.

[2]   J.F. Brennecke, E.J. Maginn, AIChE Journal, 47 (2001) 2384-2389.

[3]   A. Filippov, G. Oraedd, G. Lindblom, Biophysical Journal, 93 (2007) 3182-3190.

[4]   I.V. Polozov, K. Gawrisch, Biophysical Journal, 90 (2006) 2051–2061.

[5]   G. Oradd, P.W. Westerman, G. Lindblom, Biophys. J., 89 (2005) 315–320.

[6]   H.A. Scheidt, D. Huster, K. Gawrisch, Biophys. J., 89 (2005) 2504-2512.

[7]   K.T. Samiee, J.M. Moran-Mirabal, Y.K. Cheung, H.G. Craighead, Biophys. J., 90 (2006) 3288-3299.

[8]   J.B. Edel, M. Wu, B. Baird, H.G. Craighead, BBA - Biomembranes, 1668 (2005) 158-163.

[9]   C. Yuan, J. Furlong, P. Burgos, L.J. Johnston, Biophys. J., 82 (2002) 2526–2535.

[10]   F. Tokumasu, A.J. Jin, G.W. Feigenson, J.A. Dvorak, Biophys. J., 84 (2003) 2609–2618.

[11]   A. Choucair, M. Chakrapani, B. Chakravarthy, J. Katsaras, L.J. Johnston, Biochimica et Biophysica Acta, Biomembranes, 1768 (2007) 146-154.

[12]   M. Sanders, R. Mueller, A. Menjoge, S. Vasenkov, J. Phys. Chem. B 113 (2009) 14355–14364.

[13]   R.M. Cotts, M.J.R. Hoch, T. Sun, J.T. Markert, J. Magn. Reson., 83 (1989) 252-266.

[14]   A.R. Menjoge, J. Dixon, J.F. Brennecke, E.J. Maginn, S. Vasenkov, J. Phys. Chem. B, 113 (2009) 6353–6359.

[15]   B.-C. Lee, S.L. Outcalt, Journal of Chemical & Engineering Data, 51 (2006) 892-897.

[16]   E.D. Bates, R.D. Mayton, I. Ntai, J.H.J. Davis, J. Am. Chem. Soc., 124 (2002) 926–927.

[17]   P. Husson-Borg, V. Majer, C.G.M. F., J. Chem. Eng. Data, 48 (2003) 480–485.

[18]   R.E. Baltus, B.H. Culbertson, S. Dai, H.M. Luo, D.W.L. De Paoli, J. Phys. Chem. B, 108 (2004) 721–727.

[19]   M.B. Shiflett, A. Yokozeki, Ind. Eng. Chem. Res., 44 (2005) 4453-4464.

[20]   A.H. Jalili, A. Mehdizadeh, M. Shokouhi, A.N. Ahmadi, M. Hosseini-Jenab, F. Fateminassab, The Journal of Chemical Thermodynamics, 42 (2010) 1298-1303.

[21]   D. Morgan, L. Ferguson, P. Scovazzo, Ind. Eng. Chem. Res., 44 (2005) 4815-4823.
[22]   Y. Hou, R.E. Baltus, Ind. Eng. Chem. Res., 46 (2007) 8166-8175.
[23]   M.S. Kelkar, W. Shi, E.J. Maginn, Ind. Eng. Chem. Res., 47 (2008) 9115-9126.
[24]   M. Krutyeva, J. Kärger, Langmuir, 24 (2008) 10474-10479.
[25]   M. Krutyeva, S. Vasenkov, X. Yang, J. Caro, J. Kärger, Microporous and Mesoporous Materials, 104 (2007) 89-96.
[26]   M. Krutyeva, X. Yang, S. Vasenkov, J. Kärger, Journal of Magnetic Resonance, 185 (2007) 300-307.